Pulsed-Gradient Spin-Echo NMR Measurements of the Diffusion Coefficients of Ketones in Poly(methyl methacrylate)

X. X. Zhu and P. M. Macdonald*

Department of Chemistry and Erindale College, University of Toronto, Toronto, Ontario, Canada M5S 1A1

Received January 27, 1992; Revised Manuscript Received April 22, 1992

ABSTRACT: The self-diffusion coefficients of a series of ketone solvents, acetone (ACT), 2-butanone (MEK), 2-pentanone (MPK), 2-hexanone (MBK), 3-methyl-2-butanone (MiPK), 4-methyl-2-pentanone (MiBK), and 3,3-dimethyl-2-butanone (MtBK), mixed in various proportions with poly(methyl methacrylate) (PMMA; MW ca. 60 000) have been determined by the use of the pulsed-gradient spin-echo NMR technique. The self-diffusion coefficients of the neat solvents decrease in the order ACT > MEK > MPK > MiPK > MBK > MiBK > MtBK, according to both their increasing overall molecular length and geometric cross section. The self-diffusion coefficients of the solvents decrease in all instances with increasing PMMA concentration (e.g., from 4.65×10^{-9} to 1.46×10^{-10} m^2/s for 0–74 vol % PMMA in the case of acetone). In the concentration range investigated in this study, at a given PMMA concentration, the differences in the self-diffusion coefficients among the ketone solvents approximately parallel those differences observed with the neat solvents. The dependence of the self-diffusion coefficients on the polymer concentration is shown to agree with Fujita's free volume theory. Normalizing the extracted solvent free volume parameters with respect to the effect solvent size reveals that the solvent free volume varies inversely with the correspondng Hildebrand cohesive parameter. The size of the free volume contributed by the polymer in the solvent–polymer mixture is about 10–20% of that contributed by the solvent. We conclude that both solvent size and shape are factors determining self-diffusion coefficients, that free volume readily accounts for the effects of added polymer, and that the relative solvent free-volume contribution may be predicted using the Hildebrand cohesive parameters.

Introduction

Both practical and theoretical considerations motivate the study of small-molecule diffusion in polymeric materials. Methods employed for this purpose include vapor sorption gravimetric and radioactive tracer techniques[1] and, more recently, pulsed-gradient spin-echo (PGSE) nuclear magnetic resonance (NMR) spectroscopy.[2,3] The PGSE NMR technique enjoys certain advantages over others in that it is capable of measuring diffusion coefficients over a wide range from fast diffusion (above 10^{-6} m^2/s) to very slow diffusion (10^{-14} m^2/s).[2] The diffusing molecules are not themselves perturbed by the method, and moreover, the technique can provide individual self-diffusion coefficients from mixtures of diffusing molecules, without the need for isotopic labeling. Reports on the use of PGSE NMR for the determination of self-diffusion coefficients in polymer–solvent mixtures have been numerous and include systems such as polyisobutylene–benzene,[4] poly(methyl methacrylate)/poly(*n*-butyl methacrylate)–methyl ethyl ketone,[5] polystyrene–tetrahydrofuran,[6] and poly(isopropyl acrylate)–chloroform,[7] among many others (for review articles see von Meerwall[8] and Blum[9]).

In polymer–penetrant systems, solvent diffusion, which does not follow Fick's law, is characterized by a sharp propagation of a solvent front and considerable swelling of the polymer domain behind the front (case II diffusion). It is believed that the diffusion of small molecules occurs through the free volume in the matrix of glassy polymers. Fujita's free volume theory has related the diffusion coefficient with the free volume of the system.[10] More recently, Vrentas et al. proposed theoretical models[11,12] which relate the diffusion coefficients of the small molecules to the polymer concentration, temperature, and free volume. The theory of Thomas and Windle,[13] which explains the transport behavior of solvents in glassy polymers in terms of the diffusitivity of the solvent and the viscous flow rate of the polymer, has been successful in predicting many of the characteristics of case II diffusion.[5]

Although self-diffusion rates are quite sensitive to structural changes, to date there has been no systematic study of the effects of both solvent size and shape on diffusion of solvents in polymers. Early studies of the size effect of hydrocarbons in different cross-linked natural rubbers and in polyisobutylene determined the mutual diffusion coefficients and are summarized in the text of Crank and Park.[14] We describe here measurements of the self-diffusion coefficients of a series of ketone solvents in binary mixtures with poly(methyl methacrylate) (PMMA) obtained using PGSE NMR. The particular ketones chosen for this study (acetone, 2-butanone, 2-pentanone, 2-hexanone, and their isomers) constitute a series in which both molecular size and shape vary in a controlled and systematic fashion. We focus on how these parameters influence the self-diffusion rates as a function of polymer concentration. Furthermore, we show that the effects of solvent size and shape on self-diffusion are readily described using Fujita's free volume theory.[10]

Experimental Section

Acetone (ACT), 2-butanone (methyl ethyl ketone, MEK), 2-pentanone (methyl propyl ketone, MPK), and 3-methyl-2-butanone (methyl isopropyl ketone, MiPK) were purchased from BDH Inc. (Toronto, ON, Canada). 2-Hexanone (methyl butyl ketone, MBK), 3,3-dimethyl-2-butanone (methyl *tert*-butyl ketone, MtBK), and 4-methyl-2-pentanone (methyl isobutyl ketone, MiBK) were purchased from Aldrich (Milwaukee, WI). MiPK was further purified by refluxing with anhydrous $CaCl_2$ and redistillation prior to use. The other solvents were used without further purification. Poly(methyl methacrylate) was also purchased from Aldrich and its molecular weight was 60 000 as determined by gel permeation chromatography.

Known amounts of PMMA and the respective solvent were transferred into 5-mm NMR sample tubes, which were then sealed. The samples were heated overnight above the glass transition temperature of PMMA (105 °C), using an aluminum heating block in an oven preheated to 150–160 °C. The samples were centrifuged back and forth at least twice to ensure that

0024-9297/92/2225-4345$03.00/0

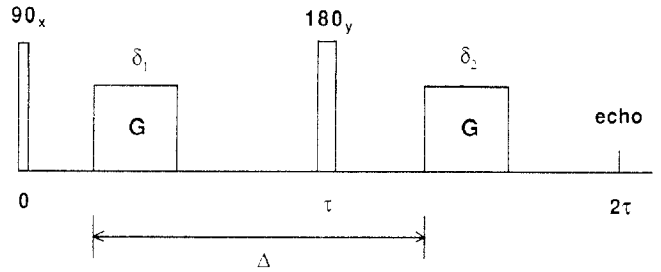

Figure 1. Pulsed-gradient spin-echo (PGSE) NMR pulse sequence. Normally, when the gradient strength is low, $\delta_1 = \delta_2$; in the case of a severe eddy current, $\delta_1 < \delta_2$.

homogeneous mixing was attained. Overheating was carefully avoided to prevent decomposition of PMMA. All the selected ketones were good solvents for PMMA and mixed well with the polymer. The mixture filled ~3 cm in height in the NMR tube. The polymer concentrations in this study ranged from 0 to ca. 70 vol %.

An MRI (magnetic resonance imaging) probe (Doty Scientific, Columbia, SC) was installed in a Chemagnetics CMX 300 NMR spectrometer operating at 300 MHz for protons. A standard PGSE sequence was used (Figure 1). In this study, the PGSE experiments were performed at 23 °C and the gradient pulse was applied to the z-direction only. It was necessary to use two levels of gradient strength, a lower level (ca. 0.2 T/m) at low polymer concentrations and a higher level (ca. 1.1 T/m) at higher polymer concentrations. The lower gradient strength was calibrated by using the diffusion coefficients of water ($D = 2.35 \times 10^{-9}$ m^2/s) and 2 vol % H_2O in D_2O ($D = 1.9 \times 10^{-9}$ m^2/s)[15,16] (see eq 1 in the following section). In the case of the higher gradient, samples of 48.2 and 64.2 wt % PMMA in acetone ($D = 1.47 \times 10^{-9}$ and 5.11×10^{-10} m^2/s, respectively, which could be measured with both the low and high gradient strength) were used as calibration standards. The precision of the measured self-diffusion coefficients of solvent was very good at low gradient strength, the error being estimated at less than 5%; at higher gradient strength, the error was larger due to the occurrence of eddy currents, but in all cases the error was less than 15%. Particulars regarding the 90° pulse lengths (24 μs), interpulse delays (10–140 ms), recycle delays (15–30 s), spectral widths (5 kHz), data size (2–4K), line broadening (5–15 Hz), and number of acquisitions (8–16 scans) are those noted in the parentheses, unless otherwise mentioned.

Molecular modeling of the ketones was performed with the use of the Alchemy II computer software (Tripos Associates, Inc.).

Results and Discussion

For isotropic diffusion in a homogeneous magnetic field, where the residual gradient G_0 is negligible, the amplitude of the NMR signal at time 2τ following the application of the PGSE pulse sequence (Figure 1) is related to the diffusion coefficient D according to[3]

$$A(2\tau) = A(0) \exp\left[-\frac{2\tau}{T_2} - (\gamma G\delta)^2 D\left(\Delta - \frac{\delta}{3}\right)\right] \qquad (1)$$

where G is the pulsed-gradient strength, δ the duration of the gradient, Δ the interval between the gradients, τ the pulse interval, γ the magnetogyric ratio, and T_2 the spin–spin relaxation time (most of the parameters are depicted in Figure 1). The effect of T_2 is constant when τ is kept constant. Therefore eq 1 can be simplified as

$$A(2\tau) = A'(0) \exp[-\gamma^2 G^2 D\delta^2(\Delta - \delta/3)] \qquad (2)$$

where $(\Delta - \delta/3)$ is the time of diffusion and the effect of T_2 is contained in the term $A'(0)$. The diffusion coefficient can be derived from the slope of a plot of the logarithm of the signal intensity as a function of $\delta^2(\Delta - \delta/3)$ once the gradient strength G is known. The latter can be obtained by calibration with a sample of known diffusion coefficient.

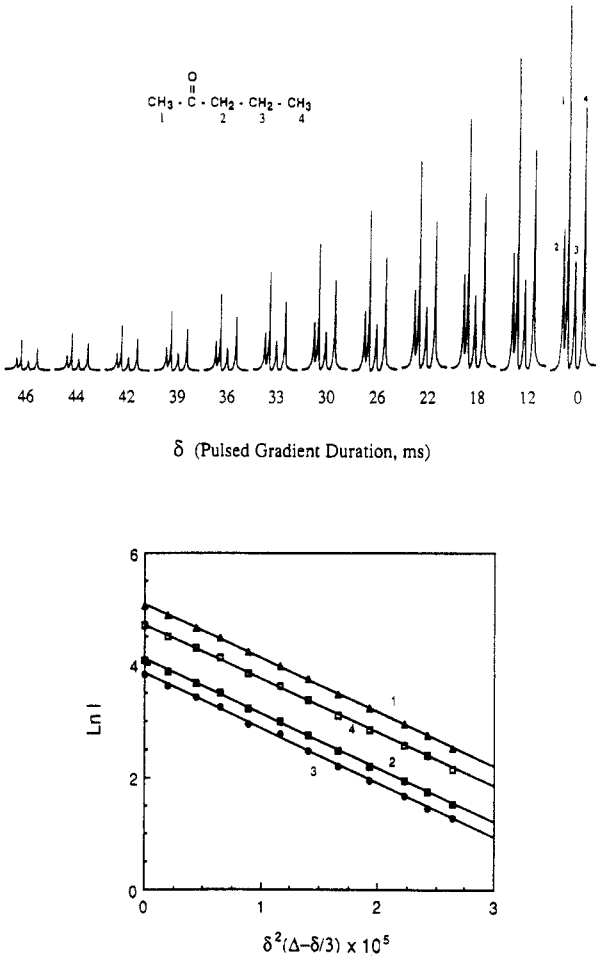

Figure 2. (A, top) Proton NMR spectra of MPK (mixture with 30 vol % PMMA), showing the attenuation of proton signals of MPK as the duration of the gradient δ increases. The absence of J-coupling in the spectra is a result of the relatively large line broadening (5 Hz) that was selected for the Fourier transform. (B, bottom) Logarithm of the NMR signal intensity (ln I) vs $\delta^2(\Delta - \delta/3)$. From the slope of the lines, the D values can be extracted according to eq 2.

Figure 2A shows the spectra obtained with a series of different values of the gradient duration δ for MPK mixed with 30 vol % PMMA. The four types of protons of MPK are all well resolved, and the assignments are depicted in the figure. The proton signals of all the ketone solvents mixed with various amounts of PMMA are all equally well resolved, and the spectra are readily assigned. The PMMA proton signals, having a much shorter T_2, do not show up in the spectra, even with the mixtures of high polymer concentrations. In Figure 2A, all the MPK proton signals show a gradual attenuation in intensity as the duration of the gradient pulse is increased. Figure 2B is a plot of the logarithm of the proton signal intensity as a function of $\delta^2(\Delta - \delta/3)$ according to eq 2. All four lines show very good linearity with coefficients of deviation greater than 0.999. They are parallel to each other, which indicates that the attenuation of the proton signals is simultaneous and uniform and that any one of the four groups of the molecule can sufficiently represent the diffusion behavior of the whole molecule.

It is experimentally facile to apply the PGSE NMR method to measure the solvent diffusion coefficients of samples of relatively low polymer concentration, where the solvent T_2 is long and large τ values (as long as 140 ms) can be employed. For samples of high polymer concentrations, two factors complicate the PGSE experiment: (1) the T_2 of the solvents becomes very short so that the

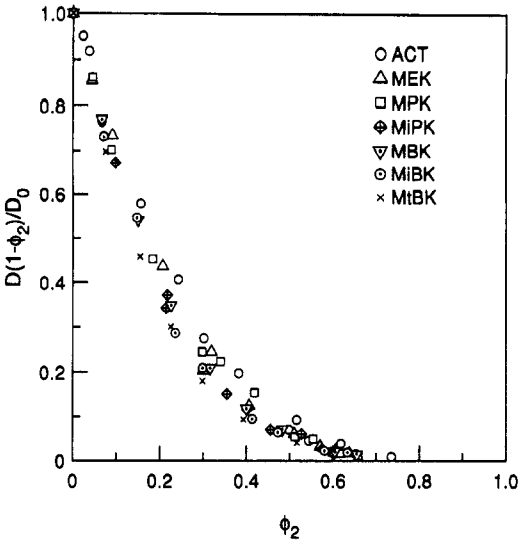

Figure 3. Normalized diffusion coefficient $D(1-\phi_2)/D_0$ plotted as a function of PMMA volume fraction.

τ value used in the PGSE NMR pulse sequence must also be kept very short; (2) the diffusion coefficient of the solvent becomes smaller and, therefore, a high gradient strength is required to attenuate the echo amplitude. The magnitude of the gradient is determined by its amplitude G and its duration δ. However, the short T_2 of the NMR signal limits in practice the duration of the gradient pulse (i.e., large δ is not possible). Therefore, in order to achieve a measurable attenuation of the NMR signal, a larger gradient amplitude has to be used. This in turn can induce severe eddy currents, which are in fact residual field gradients persisting after the gradient pulse is turned off. The presence of eddy currents can both shift the position of the echo maximum and distort its phase.[17] To overcome this problem, we have employed the method proposed by Hrovat and Wade,[18] which introduces a correction to the duration of the second gradient pulse in order to compensate for the eddy current effect. The correction along with the pulse sequence used in this study is illustrated in Figure 1. An empirical correction function, which increases the duration of second gradient pulse in a nonlinear fashion according to the duration of the first gradient pulse, was established. Details of this correction function will be published in a forthcoming article. This method helps to restore the distorted echo signal by correcting the shift of the echo maximum. However, additional phase correction is still needed for particular echoes. With application of the correction function we are able to obtain results with generally good reproducibility and precision. The very short T_2 values of the most concentrated polymer samples (over 70 vol % PMMA) remain a limitation to the use of the PGSE method to measure the diffusion coefficient.

General Dependence of Solvent Self-Diffusion Coefficients on Polymer Concentration. Blum and co-workers introduced the use of the normalized self-diffusion coefficient defined as $D(1-\phi_2)/D_0$, where D_0 is the self-diffusion coefficient of the pure solvent, ϕ_2 is the volume fraction of polymer, and the $1-\phi_2$ term corrects for the proper reference volume required by Fick's law.[9] Figure 3 illustrates the normalized self-diffusion coefficients of the seven ketone solvents in binary PMMA mixtures as a function of the volume fraction of polymer. The figure demonstrates that the normalized self-diffusion coefficients all fall along a similar curve which decreases as the PMMA volume fraction increases. There is little apparent difference between the various solvents, which

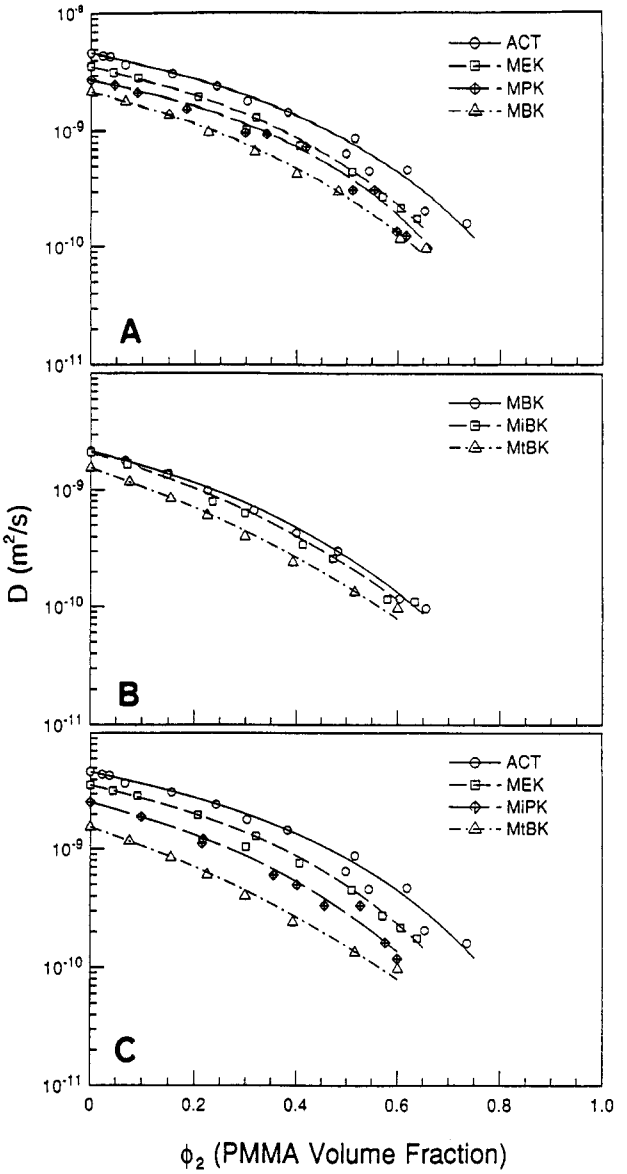

Figure 4. Self-diffusion coefficients of selected ketone solvents in PMMA as a function of PMMA volume fraction. The experimental data are fitted by Fujita's free volume theory according to eq 8. (A) Linear ketone solvents: ACT, MEK, MPK, and MBK. (B) Methyl x-butyl ketones: MBK, MiBK, and MtBK. (C) Branched ketone solvents: ACT, MEK, MiPK, and MtBK.

suggests that the decreased self-diffusion coefficient with increasing polymer volume fraction is predominantly the result of nonspecific mechanical effects rather than specific chemical interactions between the solvent and polymer. The shortcoming of such an analysis is that its sensitivity decreases as the polymer concentration increases, thereby tending to mask any differences in the behavior of different solvents. These differences are revealed when alternate means of presenting the data are employed.

Specific Effects of Molecular Structure of Solvents. Figure 4 illustrates the dependence of the solvent self-diffusion coefficient on the volume fraction of polymer for the individual ketones investigated here. In Figure 4A, we compare a series of linear ketones. It is evident that their self-diffusion coefficients decrease in the order ACT > MEK > MPK > MBK, as the length of one ketone alkyl group increases from one to four carbons. In Figure 4B, we compare three methyl butyl ketones. Their self-diffusion coefficients decrease in the order MBK > MiBK > MtBK, as the degree of branching of the butyl group increases from *n*-butyl to isobutyl to *tert*-butyl. A similar

Table I
Diffusion Coefficients and Viscosities of the Ketone Solvents at 23 °C

solvent	D (10^{-9} m^2/s)	η^a (cP)	R^b (Å)
ACT	4.65	0.321	1.45
MEK	3.58	0.407	1.49
MPK	2.76	0.484	1.62
MiPK	2.68	0.469[c]	1.72
MBK	2.17	0.602	1.66
MiBK	2.11	0.559	1.84
MtBK	1.58	0.685	2.01

[a] Assembled from the literature.[19] [b] Calculated from the Stokes–Einstein equation (eq 3). [c] Determined at 23 °C by using an Ostwald viscometer.

effect was also observed with MPK and MiPK: the self-diffusion coefficient of MiPK is systematically lower than that of MPK. In Figure 4C, we compare a series of ketones in which both molecular weight and degree of branching are altered simultaneously. The self-diffusion coefficients decrease in the order ACT > MEK > MiPK > MtBK, as the number of methyl substitutions on one of the alkyl groups is increased.

In all cases, increasing the PMMA volume fraction causes a progressive decrease in the self-diffusion coefficients of the solvents. The fitted curves in Figure 4 were generated using a simple free volume theory[10] with free volume parameters obtained as described below. One striking feature of the decrease in the self-diffusion coefficients with increasing PMMA volume fraction is that it occurs approximately in parallel for each of the solvents investigated. Thus, at a given PMMA concentration the self-diffusion coefficient for a particular ketone solvent relative to any other remains constant and may be estimated from the relative values of the diffusion coefficients of the pure solvents. A key, therefore, to understanding solvent diffusion in binary solvent–polymer mixtures lies in accounting for the differences in the diffusion coefficients of the pure solvents.

Diffusion of the Pure Solvents. The diffusion coefficients of the pure solvents decrease in the order ACT > MEK > MPK > MiPK > MBK > MiBK > MtBK. For spherical particles, the diffusion coefficient D in a medium of viscosity η can be related to the radius of the particle R through the Stokes–Einstein equation:

$$D = kT/6\pi\eta R \tag{3}$$

where k and T are the Boltzmann constant and the absolute temperature, respectively. Table I lists the diffusion coefficients measured for the pure solvent at 23 °C, along with corresponding viscosity data assembled from the literature.[19] By substitution of the viscosity and the diffusion coefficient into eq 3, the effective dynamic radius R can be calculated.

The data in Table I demonstrate that viscosity of the solvents is not an absolute predictor of the diffusion coefficient. MiBK, for instance, has both a lower viscosity and a lower diffusion coefficient than MBK, although these quantities should be inversely proportional. Clearly, molecular size and shape must be of considerable importance. The effective dynamic radius is a manifestation of the combined effects of size and shape.

The various solvent molecules studied here are by no means spherical in overall geometry, and the relationship between the effective dynamic radius and the molecular geometry deserves clarification. Using computer modeling in which both bond and torsion angles were allowed to vary, we obtained an energy-minimized conformation for each solvent molecule. From this smallest-energy conformation, the molecular dimensions (both the length and maximum and minimum cross-sectional widths) were estimated and are listed in Table II. Notice that for the linear ketones (ACT, MEK, MPK, MBK) the maximum and minimum cross-sectional widths remain constant while overall length increases progressively. For the methyl butyl ketones (MBK, MiBK, MtBK), overall length decreases while the cross-sectional width increases with increasing branching of the butyl group. For the third ketone series (ACT, MEK, MiPK, MtBK), with the exception of ACT, overall length remains constant while the cross-sectional area increases with the number of methyl substitutions. We can readily calculate an effective dynamic radius R_e for each ketone solvent provided that we approximate its molecular geometry in terms of a specific, simple geometric shape. An examination of the structures of the ketones shows that their molecular geometry might be best approximated in terms of cylindrical rods or conical sections having ellipsoidal rather than circular cross section. Equation 4 is an expression for the effective dynamic radius of a molecule having the latter geometry. It is an extension of the equation for the effective radius of molecules having a prolate shape,[20] with length L and with major and minor axial lengths d_1, d'_1 and d_2, d'_2 at either end.

Table II
Molecular Dimensions of the Ketone Solvents Obtained from Computer Modeling

			cross-section widths (Å)		
solvent	MW	max length (Å)	max	min	R_e (Å)
ACT	58.08	4.15	1.79	1.79	1.41
MEK	72.11	5.38	1.79	1.79	1.59
MPK	86.13	6.63	1.79	1.79	1.77
MiPK	86.13	5.43	4.32	1.79	1.77
MBK	100.16	7.35	1.79	1.79	1.87
MiBK	100.16	6.27	4.32	1.80	1.89
MtBK	100.16	5.46	4.32	3.78	2.11

$$R_e = \frac{(L/2)(1-(1/q))^{1/2}}{\ln\left[q^{1/2} + (q-1)^{1/2}\right]} \tag{4}$$

where

$$q = \frac{2L^2}{d_1 d'_1 + d'_1 d_2 + d_2 d'_2}$$

In the case where all the axial lengths on both ends are equal, i.e., $d_1 = d'_1 = d_2 = d'_2$, eq 4 reduces to the well-known expression describing the effective hydrodynamic radius of a cylindrical rod-shaped molecule.[20]

Values of the effective dynamic radius of the solvents calculated with eq 4 using the molecular dimensions obtained from computer modeling are listed in Table II and may be compared with those obtained by applying the Stokes–Einstein equation. For the linear ketones (ACT, MEK, MPK, MBK), we assume a cylindrical rod geometry and the agreement between the model and the experimental effective radii is generally good. However, the cylindrical rod model tends to overestimate the effective dynamic radius of the longer ketones. The ellipsoidal–conical–section model appears to be quite good for the other ketones, in that it faithfully reproduces, with small deviations, the trends in the values of the effective dynamic radius with changing molecular structure. Other geometric treatments, such as considering all the ketones to be rigid rods, spheres, or oblates, fail to yield a good correspondence between experimental and model values of R_e. The remaining discrepancies have two possible origins. First, energy-minimized molecular conformations

for the ketones were assumed in order to obtain the molecular dimensions. However, at room temperature there will be rapid trans-gauche isomerizations which tend to make the linear ketones, for examples, on average shorter and thicker than the rigid-rod approximation. Second, the effective dynamic radius calculated according to eq 4 is representative of an equivalent spherical volume. However, for nonspherical molecules, one must consider the possibility that rates of diffusion along particular axes could differ. For example, for the longer linear ketones, such as MBK, one might anticipate that diffusion parallel to the long molecular axis could occur more readily than diffusion perpendicular to the long axis. Such an effect would tend to reduce the effective dynamic radius relative to values calculated using geometric models, where no such diffusional anisotropy is presumed. Notwithstanding these uncertainties, we conclude that molecular geometry has a major impact on diffusion both in the pure solvent and in the solvent–polymer mixtures.

Free Volume Parameters. According to Fujita's modification of the Doolittle relation,[10] the diffusion coefficient is proportional to the probability that a molecule will encounter a void or free volume exceeding a given size so that

$$D = RTA \exp(-B/f) \tag{5}$$

where f is the total free volume of the system under consideration, B is the minimum hole size or jump size required for the diffusion of a given molecule or molecular segment, A is a factor depending on the size and shape of the diffusive molecule, and R and T are the gas constant and absolute temperature, respectively. The free volume of a mixed system is assumed to correspond to the sum of the fractional free volumes contributed by the individual components (e.g., solvent plus polymer) according to

$$f = f_1\phi_1 + f_2\phi_2 = f_2 + \beta\phi_1 \tag{6}$$

where ϕ_i is the volume fraction of component i having fractional free volume f_i, and where the subscripts 1 and 2 will always refer to the solvent and the polymer, respectively. Note that $\beta = f_1 - f_2$.

It is convenient to express the diffusion coefficient in a mixed system as being relative to some reference state at an identical temperature. In this instance one obtains the following expression:

$$\frac{D}{D_0} = \exp\left(-\frac{B}{f} + \frac{B}{f_0}\right) \tag{7}$$

in which D_0 and f_0 are the diffusion coefficient and fractional free volume, respectively, of the reference state. Various reference states have been employed including pure polymer,[4-10] mixed polymer–solvent,[7] and pure solvent.[5] Primarily it is a question of experimental convenience and the reliability of the diffusion data. Since we are concerned with solvent diffusion in polymer mixtures, it is natural that we choose the pure solvent as the reference state. Moreover, the precision of the PGSE NMR measurements is greatest at low polymer concentrations, as noted earlier. With the pure solvent as the reference state and B assumed as a constant throughout the concentration range, eq 7 may be transformed to

$$\left(\ln\frac{D}{D_0}\right)^{-1} = \frac{f_1}{B} - \frac{f_1^2}{B\beta}\left(\frac{1}{1-\phi_1}\right) \tag{8}$$

Thus, if free volume theory correctly accounts for the dependence of diffusion on polymer volume fraction, a plot of $1/\ln(D/D_0)$ vs $1/(1-\phi_1)$ should be linear with slope and intercept equal to $-f_1^2/(B\beta)$ and f_1/B, respectively. Figure 5 shows examples of such plots for three ketone solvents. In all cases the linearity of the fitted lines was exceptional, with values of the linear correlation coefficient, r^2, falling in the range 0.998–0.999, as determined by linear regression analysis. We conclude that free volume theory adequately describes the dependence of the solvent diffusion coefficients on the PMMA volume fraction, for all of the solvent molecular geometries. Table III lists the slopes obtained from these plots. We note that the values of f_1/B obtained from the intercepts decrease in a more-or-less continuous fashion with increasing solvent length and cross-sectional widths. However, the standard deviations of the intercepts from the fits with eq 8 are extremely large and should be interpreted only with the greatest of caution. In contrast, the slopes of the fitted lines are determined with very small standard deviations and may be interpreted with greater confidence. This difficulty with such plots has been noted previously by other workers and arises because the values of the intercepts are extremely sensitive to small deviations in the reference-state diffusion coefficient, while the slope is relatively insensitive.[10] Using the slope values listed in Table III, we generate the curves in Figure 4, overlaying the experimental self-diffusion coefficients as a function of PMMA volume fraction. The excellent correspondence between experiment and the free volume model encourages us to examine more closely the relationship between the free volume parameters and solvent molecular structure. Before this is possible, however, we need first to obtain reliable values of f_1/B, as detailed next.

It is clear from the success of the free volume approach that the decrease in the solvent self-diffusion coefficient with increasing polymer volume fraction may be attributed to the decreased overall free volume available to the solvent molecules. This can arise only when the polymer fractional

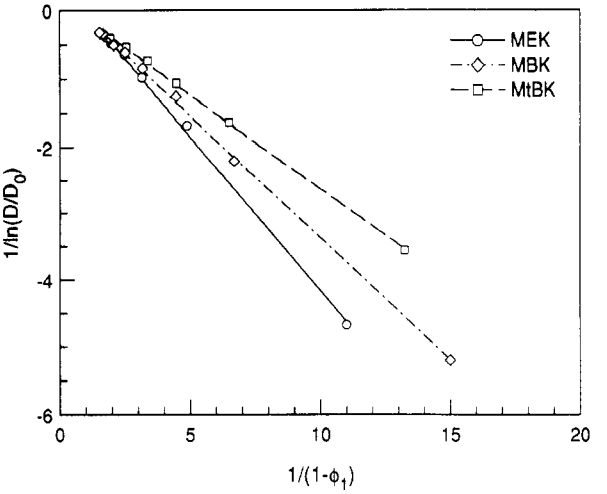

Figure 5. Plot of $[\ln (D/D_0)]^{-1}$ as a function of $(1 - \phi_1)^{-1}$ for MEK, MBK, and MtBK (pure solvent as reference point, i.e., $\phi_1^0 = 1$).

Table III
Free Volume Parameters for Ketone/PMMA Systems and Hildebrand Cohesive Parmeters for the Pure Solvents

solvent	S_8^{ib}	S_9^{ib}	δ (MPa)$^{1/2}$
ACT	−0.4595	−2.168	19.7
MEK	−0.4100	−2.355	19.3
MPK	−0.4467	−2.506	18.4
MiPK	−0.3540	−2.657	18.3
MBK	−0.3645	−2.455	17.7
MiBK	−0.3141	−2.930	17.4
MtBK	−0.2789	−3.181	16.8

[a] $S_8^i = -f_1^2/(B\beta)$, slope from eq 8. [b] $S_9^i = -B/f_1$, slope from eq 9.

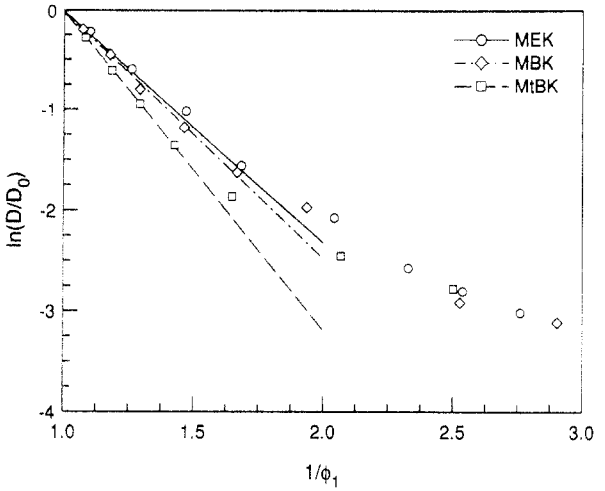

Figure 6. Plot of ln (D/D_0) as a function of ϕ_1^{-1} for MEK, MBK, and MtBK (pure solvent as reference point, i.e., $\phi_1^0 = 1$, and assuming $f_2 = 0$).

free volume is much less than that of the solvent. If it is assumed that the fractional free volume of the polymer is negligible relative to the free volume of the solvent (i.e., $f_2 \ll f_1$), then one obtains the following simplified version of eq 8

$$\ln \frac{D}{D_0} = \frac{B}{f_1} - \frac{B}{f_1}\left(\frac{1}{\phi_1}\right) \tag{9}$$

which indicates that values of ln (D/D_0) should decrease in a linear fashion as a function of $1/\phi_1$, with absolute values of both the slope and intercept equal to B/f_1, for the concentration range over which the simplifying assumption is valid. Figure 6 shows that such plots are clearly nonlinear in the range of solvent volume fractions below 0.50, so that assuming a negligible contribution of the polymer to the overall free volume is in general inappropriate. However, at solvent volume fractions of 0.70 and greater, such plots are quite nearly linear, yielding linear correlation coefficients r^2 on the order of 0.998. Moreover, the standard deviations were quite small so that the slopes provide reasonable values for the quantity B/f_1, as listed in Table III.

The free volume parameters extracted in the above fashion are always a ratio of the fractional free volume and the minimum hole size required for diffusion of a particular molecule to occur. Neither of these quantities can be expected to remain constant with changing solvent molecular structure. Although it is often assumed that B takes on a value close to unity and does not vary either with different solvents or as a function of polymer concentration, nevertheless, B is certainly a factor which depends on the molecular geometry. If we can take into account the differences in the molecular geometries of these various solvents, we can extract relative values for the fractional free volumes of the solvents that are independent of complications involving molecular shape and size. Our approach is to normalize the fractional free volumes of the solvents with respect to that of acetone according to eq 10. The normalization constant B_i/B_0

$$\frac{f_i}{f_0} = \left[\frac{f_i/B_i}{f_0/B_0}\right]\frac{B_i}{B_0} \tag{10}$$

represents the ratio of the effective hole size, B_i, for diffusion of molecule i and the effective hole size, B_0, for diffusion of acetone. We consider the effective diffusional radii obtained from the Stokes–Einstein equation (Table I) to be a good basis for normalization with respect to

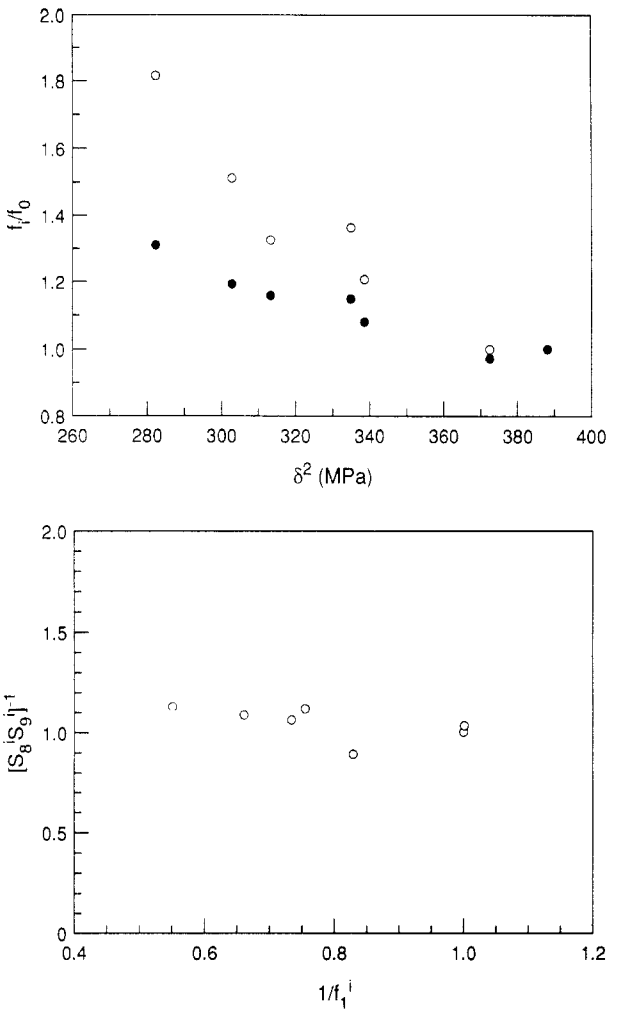

Figure 7. (A, top) Plot of the solvent cohesive pressure δ^2 vs the normalized solvent free volume f_i/f_0. Ratios of both the square (closed circles) and the cube (open circles) of the effective diffusional radii are used as the normalization constants. (B, bottom) Plot of $(S_8^i S_9^i)^{-1}$ vs $1/f_1^i$. The slope of eq 11 is the ratio of the free volume of PMMA to that of acetone.

molecular size. One might argue that it is the cross-sectional area of a hole that delimits its effective size, in which case the ratio of the square of the effective diffusional radii would represent the proper normalization constant. Alternately, if it is the hole's volume that is the deciding factor, the ratio of the cube of the effective diffusional radii would constitute the appropriate normalization constant. Figure 7A shows a plot of the normalized free volumes of the solvents as a function of the corresponding solvent cohesive pressure. Regardless of whether we employ the ratio of the square or the cube of the effective radii as the normalization constant, the normalized fractional free volumes, f_i/f_0, increase in the order ACT ≈ MEK < MPK < MBK < MiPK < MiBK < MtBK. This is virtually the inverse of the order in which the diffusion coefficients of the pure solvents (or polymer–solvent mixtures) decrease. The cohesive pressure is the square of the Hildebrand cohesive parameter[21] and represents the total strength of the intermolecular interactions of the solvent. It is, therefore, inversely proportional to the ease with which solvent molecules can be separated from one another to form cavities or free volume. Figure 7A demonstrates that there exists an inverse correlation between the normalized free volume and the corresponding solvent cohesive pressure. This finding lends credence to the free volume approach and the normalization procedure employed here. We are drawn to the conclusion

that the increase in molecular size across this series of solvents overwhelms the increase in available free volume and leads to the observed net decrease in the magnitude of the diffusion coefficients.

From the formulas for the slopes of eq 8 and 9 we can extract values for the fractional free volume of PMMA in the various solvent mixtures. Since each of the ketones is thermodynamically a good solvent for PMMA, the fractional free volume contributed by PMMA at any one polymer volume fraction should be identical for each solvent. In this case eq 11 relates the solvent and polymer

$$(S_8^i S_9^i)^{-1} = 1 - f_2/f_1^i \tag{11}$$

fractional free volumes, f_1 and f_2, respectively, with the slopes from eqs 8 and 9, S_8^i and S_9^i, respectively. Plotting $(S_8^i S_9^i)$ vs $1/f_1^i$ should yield a straight line with slope proportional to f_2, if the fractional free volume of the polymer is in fact a constant for all solvents investigated. Figure 7B demonstrates that this appears to be the case since an approximately linear relationship is produced. Thus the fractional free volume of the PMMA does appear to be approximately constant and equals approximately 10% of the fractional free volume of acetone. Note that the error in this determination is large due to the propagation of the errors in the determination of the slopes S_8^i and S_9^i.

Summary and Conclusions. We have employed PGSE NMR to determine the dependence of the self-diffusion coefficients of a series of ketone solvents on the concentration of PMMA in polymer–solvent mixtures. The diffusion coefficients of the pure solvents decrease with both increasing molecular length and geometric cross section. The effect of an increase in PMMA concentration is always to decrease the solvent self-diffusion coefficient and is readily described in terms of a simple free volume theory. The extracted free volume parameters indicate that the solvent fractional free volume is inversely proportional to the solvent cohesive pressure and exceeds the polymer fractional free volume by a factor of approximately 10. The factor most influential in determining the relative diffusion coefficient for this solvent series is the molecular size and shape.

Acknowledgment. We are grateful to Professor M. A. Winnik for his valuable suggestions and helpful discussions. This work is financially supported by an NSERC Strategic Grant from the Natural Sciences and Engineering Research Council of Canada.

References and Notes

(1) Moore, R. S.; Ferry, J. D. *J. Phys. Chem.* **1962**, *66*, 2699.
(2) Stilbs, P. *Prog. Nucl. Magn. Reson. Spectrosc.* **1987**, *19*, 1.
(3) Stejskal, E. O.; Tanner, J. E. *J. Chem. Phys.* **1965**, *42*, 288.
(4) Boss, B. D.; Stejskal, E. O.; Ferry, J. D. *J. Phys. Chem.* **1967**, *71*, 1501.
(5) Hwang, D. H.; Cohen, C. *Macromolecules* **1984**, *17*, 1679, 2890.
(6) von Meerwall, E. D.; Amis, E. J.; Ferry, J. D. *Macromolecules* **1985**, *18*, 260.
(7) Blum, F. D.; Nurairaj, B.; Padmanabhan, A. S. *J. Polym. Sci., Polym. Phys. Ed.* **1986**, *24*, 493.
(8) von Meerwall, E. D. *Adv. Polym. Sci.* **1983**, *54*, 1.
(9) Blum, F. D. *Spectroscopy* **1986**, *1*, 32.
(10) Fujita, H. *Adv. Polym. Sci.* **1961**, *3*, 1.
(11) Vrentas, J. S.; Duda, J. L.; Ling, H. C. *J. Polym. Sci., Polym. Phys. Ed.* **1985**, *23*, 275.
(12) Vrentas, J. S.; Duda, J. L.; Ling, H. C.; Hou, A. C. *J. Polym. Sci., Polym. Phys. Ed.* **1985**, *23*, 289.
(13) Thomas, N. L.; Windle, A. H. *Polymer* **1980**, *21*, 619; **1981**, *22*, 627.
(14) Crank, J.; Park, G. S. Organic Vapors above the Glass Transition Temperature. In *Diffusion in Polymers*; Academic Press: London, 1968; Chapter 3, and references therein.
(15) Mills, R. *J. Phys. Chem.* **1973**, *77*, 685.
(16) James, T. L.; McDonald, G. G. *J. Magn. Reson.* **1973**, *11*, 58.
(17) van Vaals, J. J.; Bergman, A. H. *J. Magn. Reson.* **1990**, *90*, 52.
(18) Hrovat, M. I.; Wade, C. G. *J. Magn. Reson.* **1981**, *44*, 62; **1981**, *45*, 67.
(19) Viswanath, D. S.; Natarajan, G. *Data Book on the Viscosity of Liquids*; Hemisphere Publishing Corp.: New York, 1989.
(20) Tanford, T. Transport Processes: Viscosity. In *Physical Chemistry of Macromolecules*; John Wiley & Sons Inc.: New York, 1965; Chapter 6, pp 327, 342.
(21) Barton, A. F. M. *CRC Handbook of Solubility Parameters and Other Cohesive Parameters*; CRC Press, Inc., Boca Raton, FL, 1983.

Registry No. PMMA, 9011-14-7; ACT, 67-64-1; MEK, 78-93-3; MPK, 107-87-9; MiPK, 563-80-4; MBK, 591-78-6; MtBK, 75-97-8; MiBK, 108-10-1.